

## MULTIPLE MOLECULAR INTERACTIONS IMPLICATE CONNECTIN/TITIN N2A REGION AS A MODULATING SCAFFOLD FOR P94/CALPAIN 3 ACTIVITY IN SKELETAL MUSCLE\*

Chikako Hayashi<sup>§†1</sup>, Yasuko Ono<sup>§1,2</sup>, Naoko Doi<sup>§¶</sup>, Fujiko Kitamura<sup>§</sup>, Mai Tagami<sup>§</sup>, Reiko Mineki<sup>\*\*</sup>, Takao Arai<sup>‡</sup>, Hayao Taguchi<sup>‡</sup>, Mitsuaki Yanagida<sup>†</sup>, Stephanie Hirner<sup>||</sup>, Dietmar Labeit<sup>||</sup>, Siegfried Labeit<sup>||</sup>, and Hiroyuki Sorimachi<sup>§¶12</sup>

From the <sup>§</sup>Department of Enzymatic Regulation for Cell Functions (Calpain Project), The Tokyo Metropolitan Institute of Medical Science (Rinshoken), Tokyo, Japan, <sup>‡</sup>Department of Applied Biological Science, Faculty of Science and Technology, Tokyo University of Science, Chiba, Japan, <sup>¶</sup>CREST, Japan Science and Technology (JST), Saitama, Japan, <sup>\*\*</sup>Biomedical Research Center, Juntendo University Graduate School of Medicine, <sup>||</sup>Institute für Anästhesiologie und Operative Intensivmedizin, Universitätsklinikum Mannheim, 68167 Mannheim, Germany, <sup>†</sup>Institute for Environmental and Gender Specific Medicine, Graduate School of Medicine, Juntendo University, Chiba, Japan

Running head: Calpain/connectin/MARP N2A-complex modulated by proteolysis

Address correspondence to: Yasuko Ono or Hiroyuki Sorimachi, Department of Enzymatic Regulation for Cell Functions (Calpain Project), The Tokyo Metropolitan Institute of Medical Science (Rinshoken), 3-18-22 Honkomagome, Bunkyo-ku, Tokyo 113-8613, Japan. Fax: 81-3-3823-2359; E-mail: yakoono@rinshoken.or.jp or sorimach@rinshoken.or.jp

**p94/calpain 3 is a skeletal muscle-specific Ca<sup>2+</sup>-regulated cysteine protease (calpain), and genetic loss of p94 protease activity causes muscular dystrophy (calpainopathy). In addition, a small in-frame deletion in the N2A region of connectin/titin that impairs p94/connectin interaction causes a severe muscular dystrophy (*mdm*) in mice. Since p94 via its interaction with the N2A and M-line regions of connectin becomes part of the connectin filament system that serves as a molecular scaffold for the myofibril, it has been proposed that structural and functional integrity of the p94-connectin complex is essential for myocytes health and maintenance.**

**In this study, we have surveyed the interactions made by p94 and connectin N2A inside COS7 cells. This revealed that p94 binds to connectin at multiple sites including newly identified loci in the N2A and PEVK regions of connectin. Functionally, p94–N2A interactions suppress p94 autolysis and protected connectin from proteolysis. The connectin N2A region also contains a binding site for the muscle ankyrin repeat proteins (MARPs), a protein family involved in the cellular stress responses. MARP2/Ankrd2 competed with p94 for binding to connectin and was also proteolyzed by p94.**

**Intriguingly, a connectin N2A fragment with the *mdm* deletion possessed enhanced resistance to proteases including p94, and its interaction with MARPs was weakened. Our data support a model that MARP2–p94 signaling converges within the N2A connectin segment, and that the *mdm* deletion disrupts their coordination. These results also implicate the dynamic nature of connectin molecule as a regulatory scaffold of p94 functions.**

Calpain (EC 3.4.22.18, clan CA, family C2) is a family of Ca<sup>2+</sup>-requiring and papain-like proteases comprising the products of 15 different genes in humans (1-3). Calpain is considered a modulator protease, as it modulates functions of substrates. More than 10 calpain molecules are expressed in skeletal muscle, including p94/calpain 3, a skeletal muscle-specific isoform, as well as the conventional  $\mu$ - and m-calpains, whose catalytic subunits are called calpain 1 and 2, respectively. The functions of calpain in skeletal muscle have been investigated regarding pathogenic conditions such as atrophy and muscular dystrophy (4-6), and the molecular mechanisms involved in myogenesis (7-9).

The physiological relevance of p94 to skeletal muscle integrity is an urgently pursued issue. Defective p94 protease activity by gene mutations causes a muscular dystrophy categorized as cal-

painopathy (10). The calpainopathy-type muscular dystrophy contrasts with other muscular dystrophies with regard to the mode of calpain involvement. Unlike the conventional calpains that are hyperactivated as a consequence of advanced dystrophic phenotype (*i.e.*, an aberrant increase in intracellular  $[Ca^{2+}]$ ), and, in turn, aggravate the symptoms (11), the dystrophic phenotypes of calpainopathy is caused by loss of p94 protease activity from skeletal muscle (12). Phenotypes of transgenic mice in which the p94 protease activity is manipulated in various ways showed that the regulated proteolytic action of p94 on target proteins is critical for the maintenance of skeletal muscle functions (13-16). Thus, identification of p94 substrates is a key to clarify underlying mechanisms.

One of the interesting properties of p94 is its very rapid and exhaustive autolysis in protein expression systems examined so far, whereas native p94 protein can be detected at significant quantities in skeletal muscle where it constitutes a complex with other myofibril components, especially connectin/titin (17-21). Therefore, connectin is a candidate that regulates p94 stability and activity. Two distinct regions in connectin, the N2A and C-terminus regions, have been identified as p94-binding sites by yeast two-hybrid (YTH)<sup>3</sup> screening (19,22). These interactions are thought to impede autolytic disassembly of p94, which has been demonstrated for the N2A fragment in a protease-trapping assay, a phenomenon we call “p94-trapping” (23,24). Interestingly, in primary cultures of skeletal muscle cells, p94 translocates from the M-line to the N2A region as myofibrillogenesis proceeds or as the sarcomere lengthens (25). Together, these observations suggest that p94 and connectin function as a complex in skeletal muscle cells.

The importance of connectin as a scaffold for multiple molecular interactions for both the structural and force-generating elements has been recognized (26-29). In fact, the N2A region of connectin appears to be a major site involved in signal transduction in striated muscle tissues. N-terminal to the binding site for p94 in the N2A region of connectin is a specific insertion sequence, “is”, which binds to muscle ankyrin repeat proteins (MARPs) (30) (Fig. 1A). There are three MARP paralogues: MARP1 expressed primarily in cardiac muscle (also referred to as CARP or Ankrd1),

MARP2 (Ankrd2 or Arpp) expressed primarily in skeletal muscle, and MARP3 (DARP) expressed in both muscle tissues. MARPs become strongly upregulated in myocytes under a variety of acute stresses; cardiac injury and hypertrophy (MARP1) (31-33), stretch or denervation of skeletal muscle (MARP2) (34,35), and metabolic challenge (MARP3) (36). MARP1 and 2 are upregulated in skeletal muscle in chronic pathogenic conditions such as Duchenne muscular dystrophy (37-39). MARPs are localized both in the nucleus and the sarcomere N2A region, and MARP1 and 2 also interact with nuclear factors involved in transcriptional regulation (40-42). Therefore, MARPs are thought to link nuclear transcriptional activity and sarcomere functions.

Another example of the physiological significance of the connectin N2A region is that the homozygosity of the in-frame deletion in the connectin N2A region, *Ttn<sup>mdm/mdm</sup>*, causes muscular dystrophy, *mdm*, in mice (43-45). The *mdm* deletion overlaps partially with the C-terminus of the p94 binding region and compromises the interaction between connectin I81-I83 (Fig. 1A) and p94 (23,44). Intriguingly, in *mdm* skeletal muscle, MARP1 and 2 are upregulated significantly, respectively, and their specific targeting to the sarcomeric I-band region were observed in microscopic analysis of myofibrils from *Ttn<sup>mdm/mdm</sup>* mice (44).

Most previous studies focused on single molecule such as calpain, MARP, or connectin. Here, we have focused on the simultaneous relationships among these three molecules. We examined the effect of the *mdm* deletion on properties of connectin fragments containing binding sites for both MARPs and p94. As a result, the sensitivity of N2A connectin to proteases including p94 was shown to be suppressed by the *mdm* deletion. Identification of multiple binding sites for p94 in N2A connectin, and N2A connectin and MARP2 as substrates for p94 protease activity provided a new aspect of the relationships among these molecules. We propose that p94-connectin interaction regulates and facilitates proteolytic modulation by p94 on the signaling cascade through N2A connectin and MARP2.

## Experimental Procedures

*Mouse experiments*– All procedures used for

experimental animals were approved by the Experimental Animal Care and Use Committee of the Tokyo Metropolitan Institute of Medical Science.

*cDNA constructs*– The cDNAs for human and mouse p94/calpain 3 were subcloned into expression vectors pSRD and pAS2-1 or pAS2-1c for protein expression in mammalian and yeast cells, respectively, as described previously (12,46). The yeast expression vectors for the full length and IS2 region of rat p94 were described previously (19). The mouse cDNAs encoding various regions of N2A connectin/titin and full-length MARP1, 2, and 3, were amplified by PCR from mouse skeletal muscle cDNA using *Pfu* DNA polymerase (Stratagene, La Jolla, CA). Connectin fragments were expressed as the N-terminally FLAG-tagged proteins using the expression vector pSRD (Table I). MARP1 with an N-terminal hemagglutinin (HA) or MYC epitope was expressed using pSRD. MARP2 and 3 were expressed using pcDNA3.1 as the N-terminally HA-tagged proteins (47). An expression vector pACT2 (U29899, Clontech, Mountain View, CA) was used to express cloned connectin cDNAs in a YTH assay. p94:D607A was constructed by introducing an Asp607→Ala mutation into the human p94 cDNA and inserting this into the *XbaI*–*SacI* sites of human p94 cDNA in pFastBac1 (Invitrogen, Carlsbad, CA). This mutant p94 was characterized using “p94-trapping” (23) and used for the biochemical analyses of p94 as described previously (24). cDNA for the FLAG-tagged I80-PEVK connectin fragment was subcloned into pFastBac-HTa. Enzymes used for manipulating recombinant DNA were purchased from Takara Bio (Shiga, Japan) or New England Biolabs (Ipswich, MA). Mutations described here were introduced by long PCR using *Pfu*-Turbo DNA polymerase as described previously (12). Every nucleotide of all the constructs was verified by DNA sequencing.

*Protein expression in COS7 cells and coimmunoprecipitation assay*– COS7 cells were grown in Dulbecco’s modified Eagle’s medium (Sigma, St. Louis, MO) supplemented with 10% fetal bovine serum that had been heat inactivated before use at 56°C for 30 min. Electroporation was performed using Gene Pulser (Bio Rad, Hercules, CA) according to the manufacturer’s instructions. Cells were harvested 72 h after electroporation and lysed by sonication in lysis buffer (50 mM Tris-

HCl, pH 7.5, 150 mM NaCl or CsCl, 1 mM EDTA-Na or EDTA-K, pH 8.0, and 1% TritonX-100) containing protease inhibitors [1 mM phenylmethylsulfonyl fluoride (PMSF), 0.1 mM leupeptin, and 1.5 μM aprotinin]. For cells expressing p94, 10 mM iodoacetamide was also included. The cell lysate was centrifuged at 20,630×*g* at 4°C for 15 min, and the supernatant was incubated with ANTI-FLAG M2 affinity gel (Sigma) according to the manufacturer’s instructions. For detecting the p94–connectin interaction and MARP–connectin interaction, the incubation was carried out for 2 h and 4 h, respectively. Immunoprecipitates were collected by centrifugation and were rinsed twice with lysis buffer and then twice with wash buffer (50 mM Tris-HCl, pH 7.5, 150 mM NaCl or CsCl) followed by an incubation with 3×FLAG peptide (150 ng/μl in wash buffer) for 30 min at 4°C. The supernatant was subjected to SDS-PAGE and western blot analysis.

*Western blot analysis*– Proteins were separated by SDS-PAGE and transferred onto PVDF membranes (Millipore, Billerica, MA). Membranes were probed with appropriate primary antibodies and horseradish peroxidase-coupled secondary antibodies (Nichirei, Tokyo, Japan) followed by visualization using a POD immunostaining kit (Wako, Osaka, Japan) or ECL<sup>TM</sup> Western Blotting Detection Reagent (GE, Buckinghamshire, UK).

*Antibodies*– Antibodies used in this study include anti-FLAG monoclonal antibody (clone M2, Stratagene), anti-HA monoclonal antibody (clone 6E2, Cell Signaling Technology, Danvers, MA), anti-MYC monoclonal antibody (clone 4A6, Invitrogen), anti-slow myosin heavy chain (sMHC) monoclonal antibody (clone NOQ7.5.4D, Sigma), and anti-developmental MHC (dMHC) monoclonal antibody (NCL-MHCd, Novocastra, Newcastle upon Tyne, UK). Rabbit polyclonal anti-MARP1 and MARP2 and goat anti-pIS2 antibodies were described before (23,30). An affinity-purified rabbit anti-TPALKK was generated using the keyhole limpet hemocyanin-conjugated peptide TPALKK-C (aa 8558–8563 in mouse connectin, NP\_035782), which corresponds to the N-terminal region of human connectin N2A proteolyzed by μ-calpain. Before use, the antibody was incubated on ice with peptide RAMLKKTPALKK (aa 8552–8563 in NP\_035782) to absorb the population of IgG that also recognizes the uncleaved sequence;

the final concentration of peptide was 25 mg/ml.

*Preparation of an extract from mouse skeletal and cardiac muscle*– The skeletal muscle (hamstring) and cardiac muscle tissues dissected from mice were frozen in liquid nitrogen-cooled isopentane. Cryosections from each muscle tissue, 20  $\mu$ m thick per section, were lysed in homogenizing buffer [50 mM Tris-HCl, pH 7.5, 5 mM EDTA-K, pH 8.0, and 1 mM dithiothreitol (DTT)] containing protease inhibitors as follows: 1 mM PMSF, 0.1 mM pepstatin A, and 50  $\mu$ M calpastatin peptide 42 (amino acids 140–181 of human calpastatin, NP\_001035911). The homogenate (total; T) was fractionated into the soluble fraction (supernatant; S) and insoluble fraction (pellet; P) by centrifugation at 20,630 $\times$ g for 30 min at 4°C. Equal amount of protein, 5  $\mu$ g for each sample, was separated by SDS-PAGE and subjected to western blot analysis.

*Histology and immunohistochemistry*– The posterior compartments (gastrocnemius (GC) and soleus (Sol)) of the hind limb skeletal muscles were dissected from 10-week-old *Ttn*<sup>+/+</sup> (WT) and *Ttn*<sup>mdm/mdm</sup> mice and frozen in liquid nitrogen-cooled isopentane. Serial transverse cryosections (7  $\mu$ m thick) were stained with hematoxylin and eosin followed by the examination using a light microscope (BX 60, Olympus, Tokyo, Japan). Immunofluorescence on cryosections was performed as previously described (25,30,44) using antibodies specific for MARP1, MARP2, sMHC and dMHC in combination with appropriate secondary antibodies conjugated with either Alexa Fluor 488 or 555 (Invitrogen). The nuclei were labeled with DAPI contained in a mounting medium (VECTORSHIELD Mounting Medium with DAPI, Vector laboratories, Burlingame, CA). Sections were analyzed on a laser scanning confocal microscope (LSM510, Carl Zeiss Japan, Tokyo, Japan) and the images were processed using Photoshop CS2 (Adobe Systems, San Jose, CA).

*Expression of recombinant proteins in Sf-9 cells*– Recombinant baculovirus was generated according to the protocol provided by Invitrogen, and the recombinant proteins were expressed as described previously (48). Briefly, *Spodoptera frugiperda* (Sf-9) cells were suspended in infection medium containing 1/10 vol. of each baculovirus stock solution at a concentration of  $1.0 \times 10^7$  cells/ml, left for 1 h with gentle agitation every 15 min, diluted to a concentration of  $1.0 \times 10^6$

cells/ml, and shaken at 140 rpm at 27°C for 44 to 48 h. Preparation of the cell lysate and immunoprecipitation were performed as described above for analyzing proteins expressed in COS7 cells.

*Bacterial expression and purification of recombinant proteins*– cDNA fragments corresponding to N2A region of human connectin, I80–I83 (nt 15307–16851 in X90569), and human MARP2 (nt 294–1289 in NM\_020349) were amplified by PCR from human skeletal muscle cDNA and cloned into the pET vector. Proteins were expressed in *Escherichia coli* BL21(DE3) and purified as described previously (49).

*Proteolytic assay for calpains*– One  $\mu$ g of recombinant human MARP2 was incubated with 0.25  $\mu$ g of recombinant human  $\mu$ -calpain prepared as described previously (48) in 20  $\mu$ l of incubation buffer (10 mM Tris-HCl, pH 8.0, 1 mM EDTA-K, pH 8.0, 1 mM DTT, 1 mM PMSF, 100  $\mu$ M pepstatin A) with or without 15 mM CaCl<sub>2</sub> at 30°C for 60 and 90 min. To measure p94 autolysis and proteolysis of connectin fragment activity, the lysate of Sf-9 cells expressing p94 and/or the connectin fragment was incubated with 5 mM CaCl<sub>2</sub> at 37°C. The protein concentration of cell lysates was adjusted to 0.5  $\mu$ g/ $\mu$ l. For the proteolytic assay of MARP2, recombinant His-MARP2 was added to the lysate of cells expressing p94 at a concentration of 20 ng/ $\mu$ l. The reaction was stopped by the addition of SDS sample buffer, and the sample was subjected to SDS-PAGE followed by silver staining or western blot analysis. Where indicated, protease inhibitors were added at following concentrations: 1 mM PMSF, 1 mM leupeptin, 0.1 mM E64c, and 7  $\mu$ M calpastatin domain I (Takara Bio).

*Peptide sequencing*– After SDS-PAGE, the proteins were blotted onto Pro-Blot membrane (Applied Biosystems, Foster City, CA) and then visualized by Coomassie brilliant blue G-250 staining. The target protein bands were excised and washed three times with an excess amount of 50% (v/v) methanol and then with absolute methanol. The N-terminal sequence was determined using a 491cLC protein sequencer (Applied Biosystems) according to the manufacturer's instructions.

*YTH assay*– *Saccharomyces cerevisiae* strain AH109 was transformed with a series of combination of expression vectors for various regions of connectin and p94 WT and mutants using the Fast<sup>TM</sup>-Yeast Transformation Kit (G-Biosciences/

Genotech, St. Louis, MO), according to the manufacturer's instructions. Cotransformants were selected on plates with SD medium that lacked Leu and Trp (SD-LW) and the expression of reporter genes by growth on plates that also lacked His and Ade (SD-LWHA) were measured according to the manufacturer's instructions (Clontech).

## RESULTS

*I80-PEVK connectin/titin preferentially coimmunoprecipitates with full-length p94 rather than autolyzed fragments.* We surveyed for potential p94-connectin/titin interactions by a coimmunoprecipitation thus extending our previous YTH studies (19,22,44) by a complementary approach.

p94:WT expressed in COS7 cells autolyzes very rapidly at IS1 and only a 55 kDa fragment is dominantly detectable (Fig. 1B, lane 1, anti-pIS2, closed arrowhead; Fig. 1D, arrow [1]) (20). However, when I80-PEVK, I80-PEVK(*mdm*), or I81-I83 (previously called mCN48 (23)) (Fig. 1A) was expressed with p94:WT, the full-length p94, as well as the autolyzed fragment, was detected in coimmunoprecipitates (Fig. 1B, lane 8, 9, or 12, open arrowhead). This suggests that the full-length p94 binds to the connectin fragment more efficiently than the autolyzed 55 kDa fragment does.

In apparent contrast to our previous conclusion (23), the *mdm* deletion in a connectin fragment I80-PEVK did not abolish the interaction with p94 (also confirmed when using protease inactive mutant p94:C129S(CS); data not shown). However, subsequent analysis indicated that the I80-PEVK fragment contains in addition to the previously identified p94 binding site in I82-I83 (see Fig. 1A, PpBS: primary p94 binding site) at least one additional binding site.

*Identification of novel p94 binding sites in the N2A-PEVK region of connectin.* Coimmunoprecipitation studies using p94:CS located additional binding sites for p94 within connectin's I80-is and PEVK-N regions, respectively (Fig. 1C, lane 12 and 13), which were designated as secondary p94 binding site 1 and 2 (SpBS1 and 2), as shown in Fig. 1A. Since interaction between p94:WT and I80-I81 was not detectable (Fig. 1B, lane 11), autolyzed fragments appear to be insufficient for mediating interaction with SpBS1 only. It is also possible that SpBS1 only can interact with p94 very weakly and cannot prevent p94 from autolysis.

On the other hand, I82-PEVK, in which PpBS remains intact, did not coimmunoprecipitate either p94:WT or p94:CS regardless that the FLAG-tag is N- (Fig. 1B, lane 10, or 1C, lane 5, anti-pIS2) or C-terminal (data not shown). This suggests that the connectin local structure affects its ability binding to p94.

*p94 interacts with PEVK-connectin through the proximity of the IS2 region.* Because the interaction between PEVK-N and p94:CS was detectable in the YTH assay, we examined further the binding region for SpBS2 in p94 and compared this with that for PpBS (Fig. 1D). The interaction was complicated but suggested that the SpBS2 binding region overlaps with that for PpBS in the N-terminal in the proximity of the IS2 region, with a slight extension toward the C-terminus (Fig. 1D, p94:1-600 and p94:1-594). Interestingly, the sequence encoded by exons 15 and 16 of p94 is not necessary for its interaction with SpBS2 if the C-terminal region of p94 is intact (Fig. 1D, p94:ex15-16). These data can be explained by assuming that SpBS2 binds to an intact structure in the proximity of the p94 IS2 region encoded by exon 14, which requires several extra amino acids at its N- and C-termini.

*The N2A-PEVK junction of connectin has a site that is susceptible for proteolysis.* In the course of the above experiments, some connectin fragments were detected as both full-length and a breakdown products even when these were coexpressed with p94:CS (Fig. 1C, lanes 2 and 3, anti-FLAG, closed arrowheads; Table I). In contrast, corresponding fragments with the *mdm*-deletion, *i.e.*, I80-PEVK(*mdm*) and I82-PEVK(*mdm*) lacking 83 aar, appeared to be full-length without significant breakdown products (Fig. 1B, lane 3, anti-FLAG; Fig. S1B, lane 2). The same trend was observed when I80-PEVK and I80-PEVK(*mdm*) were expressed in Sf-9 cells (see Fig. 2C, lanes 1 and 19, anti-FLAG).

The proteolytic site in I82-PEVK was determined to be the N-terminus of Ser8934 in the *mdm* deletion region (Fig. 1A, arrow [1]; Fig. S1B). Expression of various fragments encompassing Ser8934 with or without *mdm* deletion in COS7 cells suggested that fragments without *mdm* deletion are commonly proteolyzed at the same site (Fig. S1C). These results indicate that the N2A-PEVK junction is susceptible to unidentified pro-

tease(s) in COS7 and Sf-9 cells in the context of fragment structures used in this study, and that the *mdm* deletion confers resistance to this proteolytic attack.

*I80-PEVK connectin is proteolyzed by  $\mu$ -calpain in the “is” region.* Proteolysis of connectin by calpains including p94 was reported under several different experimental conditions (16,50). Thus, we co-incubated purified recombinant proteins of I80–I83 and  $\mu$ -calpain (Fig. 2A), because p94:WT is not available as a purified protein. Two proteolytic sites in the “is” region, flanking the MARP-binding region of N2A connectin, were revealed (Fig. 2B, arrows (b)/[2] and (c)/[3]).

A specific antibody for the N-terminus of the proteolyzed fragment (b) (Fig. 2B), anti-TPALKK, was generated using the corresponding mouse connectin sequence. This antibody reacted with fragment (b), but not with (a), (c), or (d) (data not shown, see **Experimental Procedures**), and was used for further analysis of connectin proteolysis.

*Connectin is proteolyzed by p94 and an unknown endogenous protease at the same site as  $\mu$ -calpain.* The detected amount of I80-PEVK decreased in the presence of coexpressed p94:WT, but not p94:CS, both in Sf-9 (data not shown) and, to a lesser extent, COS7 cells (see Fig. 5A, lane 9 vs 10, Input, anti-FLAG), suggesting that I80-PEVK is a substrate for p94. Therefore, we further examined proteolytic processes of I80-PEVK using Sf-9 and p94:D607A(DA) missense mutant (24).

Incubation of the lysate of Sf-9 cells expressing either p94:DA or p94:CS demonstrated that p94:DA has moderate  $\text{Ca}^{2+}$ -dependent activity, which was inhibited by leupeptin+E64c but not by calpastatin, representing a unique property of p94 (Fig. S2A) (24). Moreover, as in the case of p94:WT, the full-length p94:DA was predominantly coimmunoprecipitated with the connectin fragment (Fig. S2B, lane 3, open arrowhead).

Surprisingly, when the lysate of Sf-9 cells expressing I80-PEVK alone was incubated with  $\text{Ca}^{2+}$ , I80-PEVK was proteolyzed generating the 43 kDa breakdown product detectable by anti-TPALKK (Fig. 2C, lanes 1–6). This indicates that an unknown endogenous Sf-9 protease proteolyzes I80-PEVK at the same site as  $\mu$ -calpain. The proteolysis was inhibited by leupeptin+E64c+calpastatin (Fig. 2C, lane 6, anti-FLAG), but not by calpas-

tatin alone (data not shown). Considering that some calpain species are insensitive to calpastatin (51), it is possible that endogenous calpain homologue(s) in Sf-9 cells proteolyze I80-PEVK.

When p94:DA was coexpressed, proteolysis of I80-PEVK was accelerated (Fig. 2C, lanes 7–12, anti-FLAG). The peak of the 43 kDa band amount shifted to 40 min from 60 min of that without p94:DA (lane 5 vs 10, anti-TPALKK). These data suggested the involvement of p94:DA in the proteolysis of I80-PEVK directly and/or indirectly; p94:DA proteolyzes I80-PEVK in the same manner as  $\mu$ -calpain and/or activates unknown Sf-9 protease(s). In contrast, coexpression of p94:CS did not accelerate, but slightly slowed, the proteolysis of I80-PEVK (Fig. 2C, lanes 13–18). It is, thus, inferred that interaction with p94:CS protects I80-PEVK from the endogenous protease(s), and accordingly, it is likely that p94:DA binds to I80-PEVK and directly proteolyzes it when activated by  $\text{Ca}^{2+}$ .

*Differential proteolytic susceptibility of I80-PEVK and I80-PEVK(mdm).* Judging from patterns of breakdown products, proteolysis of I80-PEVK (Figs. 2B & C, (e)) probably occurs first at the N-terminus of Ser8934 generating the 62 kDa fragment (Fig. 2B, arrow [1] and fragment (f)), followed by that of Ser8558 ([2] and (g)), and then that of Gln8646/Thr8647 ([3] and (h), *ca.* 10 kDa - too small to detect).

On the other hand, I80-PEVK(*mdm*) was not proteolyzed as intensively as I80-PEVK was (Fig. 2C, anti-FLAG, lanes 19–23). The presence of coexpressed p94:DA did not significantly enhance the proteolysis, but autolysis of p94:DA with I80-PEVK(*mdm*) proceeded more slowly than with I80-PEVK (Fig. 2C, lanes 25–29 vs 7–11). Anti-TPALKK antibody faintly detected a 67 kDa band probably corresponding to the fragment (i) (Fig. 2B), generation of which was slightly enhanced and suppressed by coexpression with p94:DA and p94:CS, respectively (Fig. 2C, (i)).

Our results suggest that the “is” region of I80-PEVK becomes further sensitized to proteases including p94 after a rate-limiting proteolytic step occurred in the junction of I83-PEVK. This model would explain why I80-PEVK(*mdm*) is resistant to proteolysis. Additionally, our data suggested that p94:CS protects connectin from proteolysis at sites in the “is” region as well as in the junction of I83-

PEVK.

*Effect of connectin structure on the MARP–connectin interaction.* We next examined the MARP-binding activity of the connectin N2A fragment as another important property of connectin that could be affected by the *mdm* deletion.

First, each MARP protein had a different I80-PEVK binding activity: MARP1  $\approx$  MARP3 > MARP2 (Fig. 3A, lanes 2–4, IP, anti-HA). The interaction between connectin and MARP2, a predominant paralogue in skeletal muscle, was further weakened by deleting the region I82-PEVK (Fig. 3B, IP, lane 4 vs 5), or by introducing the *mdm* deletion (Fig. 3C, IP, anti-HA, lane 3 vs 7). The same trend was observed for the MARP1 (data not shown, and Fig. 3C, IP, anti-MYC, lane 2 vs 5). Coexpressing MARP1 with MARP2 and I80-PEVK(*mdm*), an expected condition in *Ttn<sup>mdm/mdm</sup>* skeletal muscle, decreased the amount of MARP2 (Fig. 3C, IP, anti-HA, lane 6 vs 7), but not MARP1 (anti-MYC, lane 6 vs 5), coimmunoprecipitated with the connectin fragment.

These results indicate that the region C-terminal to “is” (including those connectin sequences deleted in *mdm*) affects MARP-connectin interaction, possibly by modulating the structure of “is” surrounded by immunoglobulin domains. Additionally, MARP1 interferes with MARP2 in binding to connectin, both in WT and in *mdm*.

*Distinct subcellular distribution of MARP1 and 2 in striated muscle.* To examine whether the *in vitro* MARP-connectin interaction observed above corresponds to *in vivo* situation, expression of MARP1 and 2 in muscles from WT and *Ttn<sup>mdm/mdm</sup>* mice (N=3 for each) were compared (Fig. 3D, WT-1–3 and *mdm*-1–3, respectively).

In both WT and *Ttn<sup>mdm/mdm</sup>*, MARP1 was enriched in cardiac muscle in the insoluble myofibrillar bound fraction, consistent with its strong binding to connectin. In skeletal muscle, MARP1 was observed in insoluble fraction only in *Ttn<sup>mdm/mdm</sup>*, where MARP1 is upregulated as previously reported (44). In contrast, MARP2 was detected predominantly in the soluble fraction of skeletal muscle, and undetectable in cardiac muscle, suggesting very weak, if not zero, interaction of MARP2 with myofibrils. In *Ttn<sup>mdm/mdm</sup>* skeletal muscle, where it was robustly upregulated, MARP2 was detected slightly in the insoluble fractions as well.

These data show that MARP1 and 2 differ in

their cellular distribution in a manner consistent with our *in vitro* results, *i.e.*, connectin-binding activity is MARP1  $\gg$  MARP2. It should be noted that these molecular properties are essentially the same both in WT and *Ttn<sup>mdm/mdm</sup>* (Table II), which raises a question as to a relationship between MARP1 and MARP2 under *mdm* condition.

*Characteristics of MARP1 and 2 in the mode of induction in *Ttn<sup>mdm/mdm</sup>* skeletal muscle.* To characterize the expression of MARP1 and 2 in relation to the integrity and the fiber type in *Ttn<sup>mdm/mdm</sup>* skeletal muscle, expression of MARP1, 2, dMHC, and sMHC were simultaneously analyzed *in situ*.

As previously reported, dMHC-positive fibers were absent in WT (data not shown), whereas degeneration/regeneration of muscle fibers is apparent in 10-wk-old *Ttn<sup>mdm/mdm</sup>* skeletal muscle (Figs. 4B & D, dMHC), and abnormal morphology such as clusters of small-sized regenerating fibers and a large percentage of fibers with irregular outlines and central nuclei was apparent (Fig. 4C, HE) (45). In WT, essentially no MARP1-positive fiber was detectable (data not shown), and MARP2 was detectable only at low frequency and signal intensity (Fig. 4A), consistent with the above western blot data (Fig. 3D). Some MARP2-positive fibers were also positive for sMHC (Fig. 4A, \*).

In *Ttn<sup>mdm/mdm</sup>* muscle, MARP1-positive fibers were sparsely identified, and significantly more fibers were positive for MARP2, sMHC and/or dMHC in *mdm* than in WT (Figs. 4B–E, Table III). MARP1 was not detectable in dMHC-positive fibers (Fig. 4B), suggesting that induction of MARP1 is not significant in regenerating fibers. There was a trend that MARP1-positive fibers were also MARP2-positive and had central nuclei (Fig. 4C, arrow). Expression of MARP2 seemed independent from fiber-types specified by MHC (Figs. 4C & D). Fibers with relatively intense MARP2 signal tended to have central nuclei regardless of their fiber sizes (Fig. 4C, arrowhead). Although frequency was low, MARP1 and 2 were detected in or at the periphery of central nuclei in *Ttn<sup>mdm/mdm</sup>* (Fig. 4E). Because of low frequency, correlation between nuclear localization of MARP1/2 and the fiber type or size was not clear.

These observations demonstrate that MARP1 and 2 are not mutually exclusive as to their upregulation in *Ttn<sup>mdm/mdm</sup>* muscle. The presence of myofibers in which only MARP2 increased (Fig.

4C, arrowhead) implies different time points of action for MARP1 and 2 during regeneration of muscle, and could explain a small population of MARP2 recovered in the insoluble fraction (Fig. 3D).

*Relationships among p94, MARP2 and connectin.* Because both p94 and MARP2 show predominant expression in skeletal muscle and interaction with N2A connectin, the relationship between them may be deteriorated by the *mdm* deletion.

Less p94:CS and MARP2 coimmunoprecipitated with I80-PEVK when both were coexpressed (Fig. 5A, IP, anti-pIS2, lane 8 vs 10; anti-HA, lane 8 vs 6), indicating that p94 and MARP2 affects their interaction to connectin with each other. Further less MARP2 coimmunoprecipitated with connectin when p94:WT was used (Fig. 5A, IP, anti-HA, lanes 6–8). Considering that the amounts of immunoprecipitated I80-PEVK were similar regardless of coexpression of p94:WT or CS (Fig. 5A, IP, anti-FLAG, lanes 6–8), and that p94:WT protein existed much less than p94:CS, the observed decrease in coprecipitated MARP2 probably results from the proteolysis of MARP2 by p94:WT during their interactions with connectin.

Thus, proteolysis of MARP2 by p94 and the effect of connectin on it were further examined. First, purified recombinant MARP2 was proteolyzed  $\text{Ca}^{2+}$ -dependently in the Sf-9 lysate expressing p94:DA, which was inhibited by leupeptin+E64c, but not by calpastatin (Fig. 5B, lanes 11–15, anti-MARP2). The proteolysis was not observed in the presence of p94:CS or absence of p94 (Fig. S2C). Therefore, in addition to I80-PEVK, our studies also identified MARP2 as a substrate for p94, at least *in vitro*.

When the Sf-9 lysate coexpressing p94:DA with I80-PEVK was used, MARP2 was proteolyzed faster than without I80-PEVK (Fig. 5B, lanes 1–3 vs 11–13, anti-MARP2). Since the initial amount of p94:DA decreased when coexpressed with I80-PEVK (Fig. 5B, anti-pIS2, lane 1 vs 11), it was predicted that I80-PEVK, as a scaffold, expedites proteolysis of MARP2 by p94:DA. Results obtained with I80-PEVK(*mdm*) or I80-PEVK did not differ (Fig. 5B, lanes 6–8), indicating that I80-PEVK(*mdm*), although resistant to proteolysis itself, does not perturb proteolysis of MARP2 by p94.

*MARP2 is proteolyzed by  $\mu$ -calpain at its N-terminal region.* The proteolytic site in MARP2 cleaved by  $\mu$ -calpain corresponded to Arg77 (Fig. 6A, closed arrow, lanes 7 and 8, Fig. 6B). Previously, two connectin-binding sites in MARP2 were determined: 24–42 and 188–205 (Fig. 6B, bidirectional arrows) (30). MARP2 $\Delta$ 1–79, however, interacted with I80-PEVK as efficiently as the full-length MARP2 (Fig. 6C, lanes 2 and 3, IP, anti-FLAG), while the N-terminal MARP2 fragment, MARP2:1–76-EGFP, did not show detectable connectin-binding (data not shown). This suggests that the second ankyrin motif is sufficient for MARP2-connectin interaction under the conditions used, and that properties of MARP2 other than connectin-binding are modified by proteolysis.

## DISCUSSION

In this study, we characterized the relationships among p94, MARPs, and N2A connectin in the WT and *mdm* contexts. We found that (1) novel binding sites for p94 exist in the N-terminal (SpBS1) and C-terminal (SpBS2) regions adjacent to the previously identified site (PpBS); (2) pre-autolytic full-length p94 preferentially interacts with N2A connectin; (3) proteases including p94 and the conventional calpains proteolyze the N2A region of connectin at several sites (Fig. 7A, closed arrowheads), which is compromised in the fragments with the *mdm* deletion (Fig. 7B, open arrowheads); (4) the efficiency of binding between the connectin “is” region and MARPs is also affected by the *mdm* deletion.

Considering the huge molecular size of connectin, characteristics of subfragment might provide only limited functional insights into whole connectin molecules *in vivo*. However, our *in vitro* results demonstrate for the N2A region of connectin a propensity to undergo dynamic changes imposed intramolecularly by the local molecular structures. Identification of N2A connectin and MARP2 as possible p94 substrates implicates that the N2A region of connectin serves as a versatile scaffold for p94, which stabilizes p94 and facilitates proteolysis of MARP2 by p94 to modify its functions (Fig. 7A).

*Localization of p94 activity and targets.* Identification of sarcomeric proteins such as  $\alpha$ -actinin and connectin as p94 binding partners emphasizes the importance of these interactions to the regula-

tion of p94, especially its stability (19,21,23,25), and that p94 is also a component for signal transduction inherent in skeletal muscle structure. So far, the physiological relevance of p94 localization to the sarcomere has been unclear. Our results present three possibilities, which may be interrelated.

First, more efficient binding of the full-length p94 than its autolyzed fragment to N2A connectin can be inferred as a molecular mechanism for condensing protease activity in the proximity of p94 substrates (*i.e.*, connectin itself and MARP2) and for releasing a remnant of enzyme after completion of p94 functions in a given context (Fig. 7A).

Second, protection effect of p94:CS against proteolysis of N2A connectin may result from alteration of connectin local structures by p94 binding so that connectin is not proteolyzed spontaneously and/or randomly by yet unknown proteases, one of candidates of which is conventional calpain.

Third, the negative effect of p94:CS on the MARP2–connectin interaction could alternatively control the extent of proteolysis of MARP2 by p94 as well as its functions. One of the novel p94 binding sites of connectin, *e.g.*, SpBS1, may directly compete with MARP binding to “is”. Furthermore, the presence of several p94–connectin interactions in I80-PEVK may trigger structural changes that affect the efficiency of MARP binding.

*Activity of p94-connectin complex in Ttn<sup>mdm/mdm</sup> skeletal muscle.* The effect of the *mdm* deletion on p94 stabilities was apparently in conflict with previous results. Decrease of p94 in *Ttn<sup>mdm/mdm</sup>* skeletal muscle (43) corroborates the idea that the *mdm* deletion abrogates p94–connectin interaction required for p94 regulation. In contrast, I80-PEVK(*mdm*) was able to coprecipitate p94:WT (Fig. 1B), and autolysis of p94:DA coexpressed with I80-PEVK(*mdm*) was retarded (Fig. 2C). One interpretation is that I80-PEVK(*mdm*) can bind p94 at SpBSs, but is distinct from WT not only in its resistance to proteolysis, but also in that it hinders certain aspects of p94 protease activity.

In this context, we hypothesize that p94–connectin N2A complex represents one of functional p94 protease units; p94 as a catalytic subunit and connectin as a regulatory subunit. The observation that gait deficits found in *Ttn<sup>mdm/+</sup>* mice were restored by p94 overexpression indicates that the *mdm* deletion does not produce dominant phenotypes but causes a decrease in p94 activity (52).

*Structure of connectin fragments affecting its susceptibility to proteolysis.* The physiological relevance of connectin proteolysis previously reported (53) remains unknown to date. In cardiac myocytes, doxorubicin treatment causes degradation of connectin by m-calpain to produce a proteolyzed fragment designated T2 (54). The major proteolytic sites of connectin were suggested to be in the elastic I-band region, where N2A and its alternative splicing isoform, N2B, are located, and the adjacent PEVK region (55).  $\mu$ -calpain is also reported to interact with connectin and generate proteolyzed fragments encompassing N1 (the C-terminal to Z-line) and N2A regions (56).

Proteolysis by p94 of connectin fragments corresponding to the Z-line, PEVK, and M-line regions has also been reported (16,50). In this study, p94 was shown to target the same proteolytic site in N2A connectin as  $\mu$ -calpain. Because this proteolytic site resides in “is”, the binding site for MARP2 and for p94 itself, our results provide a decisive basis for further investigation on the effect of p94 on the MARP2–connectin interaction.

We have shown that the *mdm* deletion caused protection from proteolysis in the region of the *mdm* deletion and, rather unexpectedly, within “is”. These results indicate that proteolysis of N2A connectin proceeds step-by-step changing its structure accordingly, *i.e.*, proteolytic sites within “is” region are exposed only after the proteolysis between I83 and PEVK. One should, thus, consider that structures of connectin fragments used in experiments may affect the results as to identification of proteolytic sites.

The protease(s) responsible for spontaneous proteolysis of N2A connectin in COS7 cells has (have) not been identified; no inhibitory effect was evident for several different protease inhibitors, including leupeptin, ALLNal, E-64d, NH<sub>4</sub>Cl, Ac-YVAD-CMK, or, Z-D-CH<sub>2</sub>-DCB (data not shown).

*Relationships between MARPs and connectin with or without the mdm deletion.* Genetic studies using mice lacking MARPs suggested that MARP paralogues have functional redundancy as both structural components and signaling molecules (57). Our study, however, showed that MARPs are different in their connectin-binding activity, and, accordingly, in cellular distribution. MARP1 and 2 were shown to be differently induced under the *mdm* condition. This is consistent with previous

studies that MARP1 and 2 respond differentially depending on the quantity and/or quality of “stress” (58). Multiple cellular events should control MARP–connectin interaction in muscles (59), and whether MARPs interact with connectin as a monomer, dimer, or complex with other proteins is one of critical future issues to be investigated (49).

Studies on fiber type specificity of MARPs showed that high level expression of MARP1 is often associated with small regenerating fibers, which are labeled by embryonic MHC (corresponding to dMHC in this study), in Duchenne muscular dystrophy, but not in other muscular dystrophies (60). In *Ttn<sup>mdm/mdm</sup>* skeletal muscle, the expression of MARP1 was not detected in dMHC-positive fibers, whereas MARP2 was detected in fibers positive for sMHC or dMHC or negative for both. The same trend of MARP2 was reported in Amyotrophic lateral sclerosis (38).

Altogether, these observations suggest that the molecular mechanisms underlying the induction of MARP1 and 2 in *Ttn<sup>mdm/mdm</sup>* are distinct, and that these mechanisms are different from those in other muscular dystrophy conditions. In other words, different primary causes (*e.g.*, deletion in dystrophin or connectin) of the symptom collectively described as “dystrophy” distinguish the molecular mechanism of each symptom.

Consistent with a short life span (10-12 wk) of *Ttn<sup>mdm/mdm</sup>* mice, skeletal muscle from 10-wk-old mice examined in this study presented advanced dystrophic symptoms. The expression trend of MARP1 and 2 observed here may be related to a stage of disease progression. One of directions for the future study is comparative analysis of the time course for expression of MARP1 and 2 in relation to muscle fiber types and sizes.

*Regulated proteolysis as a modulator for muscle functions.* Proteolysis of connectin in “is” region by calpains including p94 is predicted to release connectin-MARP complex from the entire

connectin molecule, which may desensitize the connectin-MARP interaction to respond to a stretch signal transmitted as structural changes in connectin. Since a release of MARP2 N-terminal part upon proteolysis by  $\mu$ -calpain retained binding of MARP2 to connectin, the interaction of MARP2 with molecules other than connectin could be affected. In this regard, previously reported interactions of MARP2 with YB-1 or myopalladin (42,59), which is mediated by the N-terminal region of MARP2, represent good candidates.

As a condition where the proteolysis of sarcomeric components above described bears biological significance, the maintenance and remodeling of once established muscle tissues should be considered. This process must require coordinated events including proteolytic dismissal of damaged proteins and reorganization of newly synthesized proteins (61-63). Together with reported functions of muscle proteins, our data suggest that the N2A complex comprising connectin, MARP2 and p94 is capable of playing a key role in such a scenario.

This protease machinery is allowed to be dynamic and sensitive accordingly to cellular context, because of unique properties of connectin including its huge molecular size, intramolecular effects on its interaction with MARPs and on susceptibility to proteolysis, and the selective recruitment of p94 activity. Moreover, the proposed functions of MARPs in accommodating muscles to stress by regulating gene expression indicates a link between the N2A complex and the nucleus. Recent proteomic approaches also indicate that p94 is involved in the regulation of metabolism and protein synthesis (64,65). The interlocking behavior of connectin with multiple activities of skeletal muscle would assure a balanced projection of p94 activity to molecules of diverging functions. Perturbing this by, *e.g.*, the *mdm* deletion, should lead to serious dysfunction of muscles.

## REFERENCES

1. Goll, D. E., Thompson, V. F., Li, H., Wei, W., and Cong, J. (2003) *Physiol. Rev.* **83**, 731-801
2. Suzuki, K., Hata, S., Kawabata, Y., and Sorimachi, H. (2004) *Diabetes* **53 Suppl 1**, S12-18
3. Sorimachi, H., Ishiura, S., and Suzuki, K. (1997) *Biochem. J.* **328**, 721-732
4. Jackman, R. W., and Kandarian, S. C. (2004) *Am. J. Physiol. Cell Physiol.* **287**, C834-843
5. Spencer, M. J., and Mellgren, R. L. (2002) *Hum. Mol. Genet.* **11**, 2645-2655
6. Sugita, H., Ishiura, S., Suzuki, K., and Imahori, K. (1980) *Muscle Nerve* **3**, 335-339
7. Dedieu, S., Poussard, S., Mazerès, G., Grise, F., Dargelos, E., Cottin, P., and Brustis, J. J. (2004) *Exp. Cell Res.* **292**, 187-200
8. Raynaud, F., Carnac, G., Marcilhac, A., and Benyamin, Y. (2004) *Exp. Cell Res.* **298**, 48-57
9. Dedieu, S., Mazerès, G., Dourdin, N., Cottin, P., and Brustis, J. J. (2003) *J. Mol. Biol.* **326**, 453-465
10. Richard, I., Broux, O., Allamand, V., Fougerousse, F., Chiannilkulchai, N., Bourg, N., Brenguier, L., Devaud, C., Pasturaud, P., Roudaut, C., Hillaire, D., Passos-Bueno, M., Zatz, M., Tischfield, J. A., Fardeau, M., Jackson, C. E., Cohen, D., and Beckmann, J. S. (1995) *Cell* **81**, 27-40
11. Alderton, J. M., and Steinhardt, R. A. (2000) *Trends Cardiovasc. Med.* **10**, 268-272
12. Ono, Y., Shimada, H., Sorimachi, H., Richard, I., Saido, T. C., Beckmann, J. S., Ishiura, S., and Suzuki, K. (1998) *J. Biol. Chem.* **273**, 17073-17078
13. Tagawa, K., Taya, C., Hayashi, Y., Nakagawa, M., Ono, Y., Fukuda, R., Karasuyama, H., Toyama-Sorimachi, N., Katsui, Y., Hata, S., Ishiura, S., Nonaka, I., Seyama, Y., Arahata, K., Yonekawa, H., Sorimachi, H., and Suzuki, K. (2000) *Hum. Mol. Genet.* **9**, 1393-1402
14. Spencer, M. J., Guyon, J. R., Sorimachi, H., Potts, A., Richard, I., Herasse, M., Chamberlain, J., Dalkilic, I., Kunkel, L. M., and Beckmann, J. S. (2002) *Proc. Natl. Acad. Sci. U. S. A.* **99**, 8874-8879
15. Richard, I., Roudaut, C., Marchand, S., Baghdiguian, S., Herasse, M., Stockholm, D., Ono, Y., Suel, L., Bourg, N., Sorimachi, H., Lefranc, G., Fardeau, M., Sebille, A., and Beckmann, J. S. (2000) *J. Cell Biol.* **151**, 1583-1590
16. Kramerova, I., Kudryashova, E., Tidball, J. G., and Spencer, M. J. (2004) *Hum. Mol. Genet.* **13**, 1373-1388
17. Maruyama, K. (1976) *J. Biochem.* **80**, 405-407
18. Tokuyasu, K. T., and Maher, P. A. (1987) *J. Cell Biol.* **105**, 2795-2801
19. Sorimachi, H., Kinbara, K., Kimura, S., Takahashi, M., Ishiura, S., Sasagawa, N., Sorimachi, N., Shimada, H., Tagawa, K., Maruyama, K., and et al. (1995) *J. Biol. Chem.* **270**, 31158-31162
20. Sorimachi, H., Toyama-Sorimachi, N., Saido, T. C., Kawasaki, H., Sugita, H., Miyasaka, M., Arahata, K., Ishiura, S., and Suzuki, K. (1993) *J. Biol. Chem.* **268**, 10593-10605

21. Kinbara, K., Ishiura, S., Tomioka, S., Sorimachi, H., Jeong, S. Y., Amano, S., Kawasaki, H., Kolmerer, B., Kimura, S., Labeit, S., and Suzuki, K. (1998) *Biochem. J.* **335**, 589-596
22. Kinbara, K., Sorimachi, H., Ishiura, S., and Suzuki, K. (1997) *Arch. Biochem. Biophys.* **342**, 99-107
23. Ono, Y., Torii, F., Ojima, K., Doi, N., Yoshioka, K., Kawabata, Y., Labeit, D., Labeit, S., Suzuki, K., Abe, K., Maeda, T., and Sorimachi, H. (2006) *J. Biol. Chem.* **281**, 18519-18531
24. Ono, Y., Hayahi, C., Doi, N., Tagami, M., and Sorimachi, H. (2008) *FEBS Lett.* *in press*
25. Ojima, K., Ono, Y., Doi, N., Yoshioka, K., Kawabata, Y., Labeit, S., and Sorimachi, H. (2007) *J. Biol. Chem.* **282**, 14493-14504
26. Maruyama, K. (1997) *FASEB J.* **11**, 341-345
27. Centner, T., Fougereousse, F., Freiburg, A., Witt, C., Beckmann, J. S., Granzier, H., Trombitas, K., Gregorio, C. C., and Labeit, S. (2000) *Adv. Exp. Med. Biol.* **481**, 35-49, 50-52
28. Tskhovrebova, L., and Trinick, J. (2003) *Nat. Rev. Mol. Cell Biol.* **4**, 679-689
29. Miller, M. K., Granzier, H., Ehler, E., and Gregorio, C. C. (2004) *Trends Cell Biol.* **14**, 119-126
30. Miller, M. K., Bang, M. L., Witt, C. C., Labeit, D., Trombitas, C., Watanabe, K., Granzier, H., McElhinny, A. S., Gregorio, C. C., and Labeit, S. (2003) *J. Mol. Biol.* **333**, 951-964
31. Aihara, Y., Kurabayashi, M., Saito, Y., Ohyama, Y., Tanaka, T., Takeda, S., Tomaru, K., Sekiguchi, K., Arai, M., Nakamura, T., and Nagai, R. (2000) *Hypertension* **36**, 48-53
32. Carson, J. A., Nettleton, D., and Reecy, J. M. (2002) *FASEB J.* **16**, 207-209
33. Chen, Y. W., Nader, G. A., Baar, K. R., Fedele, M. J., Hoffman, E. P., and Esser, K. A. (2002) *J. Physiol.* **545**, 27-41
34. Kemp, T. J., Sadosky, T. J., Saltisi, F., Carey, N., Moss, J., Yang, S. Y., Sassoon, D. A., Goldspink, G., and Coulton, G. R. (2000) *Genomics* **66**, 229-241
35. Tsukamoto, Y., Senda, T., Nakano, T., Nakada, C., Hida, T., Ishiguro, N., Kondo, G., Baba, T., Sato, K., Osaki, M., Mori, S., Ito, H., and Moriyama, M. (2002) *Lab. Invest.* **82**, 645-655
36. Ikeda, K., Emoto, N., Matsuo, M., and Yokoyama, M. (2003) *J. Biol. Chem.* **278**, 3514-3520
37. Bakay, M., Zhao, P., Chen, J., and Hoffman, E. P. (2002) *Neuromuscul. Disord.* **12 Suppl 1**, S125-141
38. Nakamura, K., Nakada, C., Takeuchi, K., Osaki, M., Shomori, K., Kato, S., Ohama, E., Sato, K., Fukayama, M., Mori, S., Ito, H., and Moriyama, M. (2002) *Pathobiology* **70**, 197-203
39. Nakada, C., Oka, A., Nonaka, I., Sato, K., Mori, S., Ito, H., and Moriyama, M. (2003) *Pathol. Int.* **53**, 653-658
40. Jeyaseelan, R., Poizat, C., Baker, R. K., Abdishoo, S., Isterabadi, L. B., Lyons, G. E., and Kedes, L. (1997) *J. Biol. Chem.* **272**, 22800-22808
41. Zou, Y., Evans, S., Chen, J., Kuo, H. C., Harvey, R. P., and Chien, K. R. (1997) *Development* **124**, 793-804

42. Kojic, S., Medeot, E., Guccione, E., Krmac, H., Zara, I., Martinelli, V., Valle, G., and Faulkner, G. (2004) *J. Mol. Biol.* **339**, 313-325
43. Garvey, S. M., Rajan, C., Lerner, A. P., Frankel, W. N., and Cox, G. A. (2002) *Genomics* **79**, 146-149
44. Witt, C. C., Ono, Y., Puschmann, E., McNabb, M., Wu, Y., Gotthardt, M., Witt, S. H., Haak, M., Labeit, D., Gregorio, C. C., Sorimachi, H., Granzier, H., and Labeit, S. (2004) *J. Mol. Biol.* **336**, 145-154
45. Heimann, P., Menke, A., Rothkegel, B., and Jockusch, H. (1996) *Cell Tissue Res.* **283**, 435-441
46. Herasse, M., Ono, Y., Fougerousse, F., Kimura, E., Stockholm, D., Beley, C., Montarras, D., Pinset, C., Sorimachi, H., Suzuki, K., Beckmann, J. S., and Richard, I. (1999) *Mol. Cell Biol.* **19**, 4047-4055
47. Sato, N., Kawahara, H., Toh-e, A., and Maeda, T. (2003) *Mol. Cell Biol.* **23**, 6662-6671
48. Ono, Y., Kakinuma, K., Torii, F., Irie, A., Nakagawa, K., Labeit, S., Abe, K., Suzuki, K., and Sorimachi, H. (2004) *J. Biol. Chem.* **279**, 2761-2771
49. Witt, S. H., Labeit, D., Granzier, H., Labeit, S., and Witt, C. C. (2005) *J. Muscle Res. Cell Motil.* **26**, 401-408
50. Taveau, M., Bourg, N., Sillon, G., Roudaut, C., Bartoli, M., and Richard, I. (2003) *Mol. Cell Biol.* **23**, 9127-9135
51. Laval, M., and Pascal, M. (2002) *Biochim. Biophys. Acta.* **1570**, 121-128
52. Huebsch, K. A., Kudryashova, E., Wooley, C. M., Sher, R. B., Seburn, K. L., Spencer, M. J., and Cox, G. A. (2005) *Hum. Mol. Genet.* **14**, 2801-2811
53. Suzuki, A., Kim, K., and Ikeuchi, Y. (1996) *Adv. Biophys.* **33**, 53-64
54. Lim, C. C., Zuppinger, C., Guo, X., Kuster, G. M., Helmes, M., Eppenberger, H. M., Suter, T. M., Liao, R., and Sawyer, D. B. (2004) *J. Biol. Chem.* **279**, 8290-8299
55. Helmes, M., Trombitas, K., and Granzier, H. (1996) *Circ. Res.* **79**, 619-626
56. Raynaud, F., Fernandez, E., Coulis, G., Aubry, L., Vignon, X., Bleimling, N., Gautel, M., Benyamin, Y., and Ouali, A. (2005) *FEBS J.* **272**, 2578-2590
57. Barash, I. A., Bang, M. L., Mathew, L., Greaser, M. L., Chen, J., and Lieber, R. L. (2007) *Am. J. Physiol. Cell Physiol.* **293**, C218-C227
58. Hentzen, E. R., Lahey, M., Peters, D., Mathew, L., Barash, I. A., Friden, J., and Lieber, R. L. (2006) *J. Physiol.* **570**, 157-167
59. Bang, M. L., Mudry, R. E., McElhinny, A. S., Trombitas, K., Geach, A. J., Yamasaki, R., Sorimachi, H., Granzier, H., Gregorio, C. C., and Labeit, S. (2001) *J. Cell Biol.* **153**, 413-427
60. Nakada, C., Tsukamoto, Y., Oka, A., Nonaka, I., Sato, K., Mori, S., Ito, H., and Moriyama, M. (2004) *Pathobiology* **71**, 43-51
61. Zak, R., Martin, A. F., Prior, G., and Rabinowitz, M. (1977) *J. Biol. Chem.* **252**, 3430-3433
62. Taylor, R. G., Papa, I., Astier, C., Ventre, F., Benyamin, Y., and Ouali, A. (1997) *J. Muscle Res. Cell Motil.* **18**, 285-294

63. Bassaglia, Y., Cebrian, J., Covan, S., Garcia, M., and Foucrier, J. (2005) *Exp. Cell Res.* **302**, 221-232
64. Cohen, N., Kudryashova, E., Kramerova, I., Anderson, L. V., Beckmann, J. S., Bushby, K., and Spencer, M. J. (2006) *Proteomics* **6**, 6075-6084
65. Ono, Y., Hayashi, C., Doi, N., Kitamura, F., Shindo, M., Kudo, K., Tsubata, T., Yanagida, M., and Sorimachi, H. (2007) *Biotechnol. J.* **2**, 565-576

## FOOTNOTES

\*We are grateful to Dr Kimie Murayama in Juntendo University, and to all “Calpain Project” members for experimental support and valuable discussion. This work was supported in part by research grants MEXT.KAKENHI 17028055 and 18076007 (to H.S.), JSPS.KAKENHI 18770124 (to Y.O.), 18380085 (to H.S.), Research Grant 17A-10 for Nervous and Mental Disorders from the Ministry of Health, Labour and Welfare, and the Takeda Science Foundation research grant (to H.S.), the SFB753 and the DFG (La668/9-1+11-1 to S.L. and La1619/1-1 to D.L.).

<sup>1</sup>These authors contributed equally to this work.

<sup>2</sup>To whom correspondence should be addressed: Department of Enzymatic Regulation for Cell Functions (Calpain Project), The Tokyo Metropolitan Institute of Medical Science (Rinshoken), 3-18-22 Honkomagome, Bunkyo-ku, Tokyo 113-8613, Japan. Tel.: 81-3-3823-2181; Fax: 81-3-3823-2359; E-mail: yakoono@rinshoken.or.jp or sorimach@rinshoken.or.jp

<sup>3</sup>The abbreviations used are: E64c, [L-3-trans-carboxyoxirane-2-carbonyl] L-leucine(3-methylbutyl) amide; *mdm*, muscular dystrophy with myositis; HA, hemagglutinin; I8x, immunoglobulin motif No. 8x in the I-band region of connectin/titin; “is”, intervening sequence region in N2A connectin/titin; MARP, muscle ankyrin-repeat protein; p94, muscle-specific calpain (calpain 3); dMHC and sMHC, developmental and slow-type isoforms of myosin heavy chain; PEVK, Pro, Glu, Val, and Lys-rich region; PMSF, phenylmethylsulfonyl fluoride; PpBS and SpBS, primary and secondary p94 binding site, respectively; WT, wild type; CS, C129S protease deficient mutant; DA, D607A missense mutant; YTH, yeast two-hybrid.

## FIGURE LEGENDS

**Fig. 1. Interaction between p94 and the connectin N2A-PEVK region.** *A*, Schematic structure of the N2A-PEVK connectin/titin region and constructs used in this study. Numbers correspond to aa in the mouse connectin, NP\_035782. *Horizontal bars* above connectin indicate the binding regions for MARP (=“is”) and p94 (=PpBS, primary p94 binding site) identified previously by YTH. The 83-aa span deleted in *mdm* is indicated by a *bracket*. “I80”–“I83”, “is”, and “PEVK” indicate the 80<sup>th</sup> to 83<sup>rd</sup> immunoglobulin (IG) motifs, a specific insertion sequence, and a region rich in Pro, Glu, Val, and Lys, respectively, in the connectin I-band region. *Vertical arrows* [1]–[3] and *bidirectional arrows* indicate the proteolytic sites and p94 binding sites (SpBS, secondary p94 binding site), respectively, identified in this study. The ability of each fragment to coimmunoprecipitate p94:WT or p94:CS and its susceptibility to endogenous proteolysis at the junction of I83 and PEVK are summarized on the right. NA, not applicable; ND, not determined. *B*, Connectin constructs indicated and p94:WT were coexpressed in COS7 cells (Input) and immunoprecipitated by anti-FLAG (IP). Note that the full-length 94 kDa band for p94:WT (*open arrowhead*), was hardly detectable in the cell lysate before immunoprecipitation (lanes 1-6), but was efficiently coim-

munoprecipitated with I80-PEVK, I80-PEVK(*mdm*), and I81-I83(mCN48) (lanes 8, 9, and 12). *C*, Mapping of novel p94 binding sites using protease-inactive mutant p94:CS. p94:CS was coimmunoprecipitated with PEVK-N and I80-is (lanes 12 and 13), and these regions were designated as SpBS1 and 2 as in *A*. *D*, Summary of YTH assays for binding of p94 to two different regions of connectin, I81-I83 (PpBS) and PEVK-N (SpBS2). *Arrows* [1]–[3] refer to p94 autolytic sites. The region containing IS2 is enlarged to show the sequences encoded by exons 14 to 16.

**Fig. 2. Proteolysis of N2A connectin by calpain.** *A*, Recombinant human connectin fragment, His-I80–I83, and  $\mu$ -calpain were co-incubated in the presence of  $\text{Ca}^{2+}$  with amounts indicated. *Arrowhead* (a) and *arrows* (b)–(d) indicate the full-length (69 kDa) and proteolyzed fragments as shown in *B*. *B*, Proteolytic fragments of I80-I83 are schematically summarized. *Bidirectional arrows* (a)–(d) correspond to (a)–(d) in *A*. Proteolytic sites for  $\mu$ -calpain are indicated according to mouse connectin, NP\_035782. The *closed arrowhead* indicates another proteolytic site for calpain determined previously (48). The span of full-length and proteolytic fragments of I80-PEVK or I80-PEVK(*mdm*) are represented by *bidirectional arrows* (e)–(i); the antibodies used to detect them in Sf-9 cell lysates (Fig. 2C) are shown on the right. The anti-TPALKK antibody was generated against the mouse connectin sequence corresponding to the N-terminus of proteolyzed fragment (b) (*bracket*). *Horizontal bars* indicate binding sites for MARPs (is) and p94 (SpBS1 and PpBS). *C*, Expression of I80-PEVK or I80-PEVK(*mdm*) in Sf-9 cells without (-) or with p94:DA or p94:CS. The cell lysates were incubated for indicated times in the presence of 1 mM PMSF and 5 mM  $\text{CaCl}_2$  at 37°C. Note that I80-PEVK, but not I80-PEVK(*mdm*), was proteolyzed by endogenous protease(s) in a  $\text{Ca}^{2+}$ -dependent manner (anti-FLAG and anti-TPALKK, lanes 1–5), which was accelerated by coexpressing p94:DA (lanes 7–11) or attenuated by p94:CS (lanes 13–17). Proteolysis of I80-PEVK was inhibited in the presence of calpastatin, leupeptin, and E64c (lanes 6, 12, and 18) but not by calpastatin alone (not shown). *Arrows* (e)–(g) and (i) correspond to fragments labeled in Fig. 2B. \*, nonspecific signals.

**Fig. 3. Differences in connectin-binding activity and subcellular localization among MARPs.** *A*, Combination of FLAG-tagged I80-PEVK and HA-tagged MARP1–3 as indicated were coexpressed in COS7 cells (Input) for a coimmunoprecipitation assay (IP). MARP1 and 3 coimmunoprecipitated more efficiently with the I80-PEVK fragment than did MARP2. *B*, C-terminal non-binding region of connectin affected binding to MARP2. Note that both I80-I81 (lane 4) and I80-PEVK (lane 5) contain MARP2 binding site, “is”, but showed distinct binding ability to MARP2. *C*, MYC-MARP1 or HA-MARP2, or both, were coexpressed with FLAG-tagged I80-PEVK or I80-PEVK(*mdm*) in COS7 cells as indicated combinations. We noted that less MARP1 or MARP2 coimmunoprecipitated with I80-PEVK(*mdm*) than with I80-PEVK (lanes 2 and 5, IP, anti-MYC; lanes 3 and 7, IP, anti-HA). The interaction between MARP2 and I80-PEVK or I80-PEVK(*mdm*) was strongly suppressed by coexpression with MARP1, whereas MARP1 was not affected (lanes 6 and 7, anti-HA; lanes 5 and 6, anti-MYC). *D*, The amount of MARP1 and 2 in whole tissue homogenates (T), soluble (S), and insoluble fractions (P) of skeletal and cardiac muscles from three independent wild type (WT-1 to 3) or *Ttn*<sup>*mdm/mdm*</sup> mice (*mdm*-1 to 3) was examined using anti-MARP1 and MARP2 antibodies. For summary of the results, see Table II. *Open* and *closed arrowheads* in *A*–*C*, the full-length and the N-terminal proteolyzed fragments of FLAG-connectin, respectively.

**Fig. 4. Expression of MARP1 and MARP2 in WT and *Ttn*<sup>*mdm/mdm*</sup> mouse skeletal muscle.** MARP1 or 2 (red) and slow (sMHC) or developmental MHC (dMHC) isoform (green) were detected by double-labeled immunofluorescence on sections of posterior parts of hind limbs from WT (*A*) and *Ttn*<sup>*mdm/mdm*</sup> (*B*–*E*) mice using specific antibodies. Nuclei were stained with DAPI (blue). Representative images were selected. *A*, In WT muscle, fibers faintly positive for MARP2 were identified at a low frequency. Some of these fibers were sMHC-positive (\*). *B*, In the corresponding area of *Ttn*<sup>*mdm/mdm*</sup> muscle, fibers expressing MARP1 were sparsely observed, where central nuclei were also identified (*arrowhead*). Expression of MARP1 was not detected in fibers expressing dMHC (\*). *C*, Two serial sections were stained with anti-

MARP1, 2, and sMHC. Fibers expressing MARP2 and/or sMHC were observed more frequently compared to WT. Expression of MARP1 and 2 is not mutually exclusive, and is independent of the muscle fiber types. Examples of combination of MARP1, 2, and sMHC expressed in the same fiber were shown by *arrows* (+, +, -), *arrowheads* (-, +, -), and *asterisks* (-, +, +). *D*, Expression of MARP2 was observed both in dMHC-positive (\*) and -negative fibers (*arrowheads*). *E*, Occasionally, MARP1 and MARP2 were localized in or at the periphery of central nuclei in *Ttn<sup>mdm/mdm</sup>* myofibers. *Bars*, 20  $\mu\text{m}$ .

**Fig. 5. Effects of p94 protease activity on MARP2.** *A*, p94:WT or p94:CS was coexpressed with FLAG-I80-PEVK and/or HA-MARP2 in COS7 cells for a coimmunoprecipitation assay as described in the previous Figs. Note that coexpression of p94:WT decreased MARP2 in both the cell lysate and coimmunoprecipitate (lanes 3 and 7, anti-HA), whereas p94:CS decreased MARP2 only in the coimmunoprecipitate (lanes 6 and 8, anti-HA). *B*, The lysate of Sf-9 cells expressing p94:DA without (-) or with I80-PEVK or I80-PEVK(*mdm*) was incubated with recombinant His-MARP2 in the presence of 5 mM  $\text{Ca}^{2+}$  and 1 mM PMSF at 37°C. Autolysis of p94:DA and proteolysis of MARP2 and/or I80-PEVK were inhibited completely by leupeptin and E64c (lanes 5, 10, and 15), but not by calpastatin (lanes 4, 9, and 14). *Open* and *closed arrowheads* indicate the full-length and autolyzed fragments of p94, respectively.

**Fig. 6. Effect of proteolysis by  $\mu$ -calpain on the MARP2–connectin interaction.** *A*, Recombinant MARP2 was proteolyzed by recombinant human  $\mu$ -calpain under indicated conditions. *Open* and *closed arrowheads* indicate  $\mu$ -calpain and its autolyzed fragment, respectively. *Open* and *closed arrows* indicate the full-length and the proteolyzed fragments of MARP2, respectively. *B*, The N-terminal sequence of MARP2 proteolyzed by  $\mu$ -calpain was determined to be R77 (aar in Q9GZV1) (*arrow*). NLS, nuclear localization signal; PEST, a region rich in Gln, Ser, and Thr flanked by Pro, which is considered to be susceptible for calpain proteolysis; ANK, ankyrin repeat motif. *C*, HA-MARP2 $\Delta$ 1–79 coimmunoprecipitated I80-PEVK as efficiently as the full-length MARP2 did. *Open* and *closed arrows*, HA-MARP2 and HA-MARP2 $\Delta$ 1–79, respectively. \*, nonspecific signals.

**Fig. 7. A hypothetical scheme of the molecular complex at the N2A connectin.** *A*, Summary of the N2A region in connectin and the relationships between p94 and MARPs in WT skeletal muscle. MARP2 binds to the connectin “is” region, which is suppressed by the interaction between p94 and connectin. At least three regions in N2A connectin are involved as scaffolds in p94-connectin complex. *Closed arrowheads* indicate the proteolytic sites in N2A connectin and MARP2 determined in this study. Unproteolyzed connectin orchestrates multiple signal transductions (*upper*). Activation of proteolytic machinery, *i.e.*, p94-connectin complex, results in proteolyzed connectin fragments whose interaction with MARP2 as well as other functions are modulated (*lower*). MARP2 is also proteolyzed to generate the free N-terminal fragment, MARP2-(N), and the C-terminal connectin-associated fragment, MARP2-(C). Dissociation from connectin prompts autolysis of p94 to terminate its activity. Coordination of these reactions prevents aggravation of muscle damage triggered under various physiological conditions. *B*, Stalled proteolysis incited by the *mdm* deletion in connectin. In *Ttn<sup>mdm/mdm</sup>* skeletal muscle, expression of MARP1 and 2 is upregulated as a result of aberrant signal transduction by connectin with the *mdm* deletion. When MARP1 and 2 are coexpressed in the same muscle fiber, “is” is dominantly occupied by MARP1. On the other hand, several fibers express only MARP2, which binds to “is” without interference by MARP1 and is subjected to proteolysis. The *mdm* deletion impairs the nature of connectin as a substrate for proteases, and distorts interaction between p94 and connectin, which compromises functions of p94-connectin complex. These abnormalities cause deficits in cellular response to muscle damage, *i.e.*, dystrophic symptoms observed in *Ttn<sup>mdm/mdm</sup>* skeletal muscle. *Open arrowheads* indicate proteolytic sites in connectin apparently invalidated by the *mdm* deletion. *Wavy lines* represent distorted interaction between p94 and connectin.

**Table I. Fragments from mouse connectin N2A-PEVK region used in this study**

<b>Construct</b>	<b>Amino acid residue in NP_035782</b>	<b>Calculated molecular weight (kDa)<sup>a</sup></b>	<b>Observed molecular weight (kDa)<sup>b</sup></b>
I80-PEVK	8463–9137	80	97, 60 <sup>c</sup>
I80-PEVK( <i>mdm</i> )	8463–8894/8978–9137	70	85
I80–I83Δ	8463–8895	52	58
I80–I82	8463–8826	43	45, 35
I80–I81	8463–8738	33	33, 26
I80–is	8463–8655	24	26
I81–I83(mCN48)	8613–8915	37	39
I81-I83/PEVK	8613–8998	46	47, 36
I81-I83/PEVK( <i>mdm</i> )	8613–8894/8978–8998	37	42
I81–I83:I8931term	8613–8930	38	39
I81–I83:I8951term	8613–8950	41	41
I82-PEVK	8739–9137	48	66, 31
PEVK-N	9089–9526	52	99

<sup>a</sup> Additional 1.4 kDa for the N-terminal FLAG-tag is included. <sup>b</sup> For proteins expressed in COS7 cells with the N-terminal FLAG-tag. <sup>c</sup> The lower molecular weight corresponds to a proteolytic fragment.

Table II. Cellular distribution of MARPs

		MARF1		MARF2	
		Sup	Ppt	Sup	Ppt
Skeletal muscle	WT <sup>a</sup>	- <sup>c</sup>	-	±	-
	<i>mdm</i> <sup>b</sup>	-	++	+++	+
Cardiac muscle	WT	-	+	-	-
	<i>mdm</i>	-	++	-	-

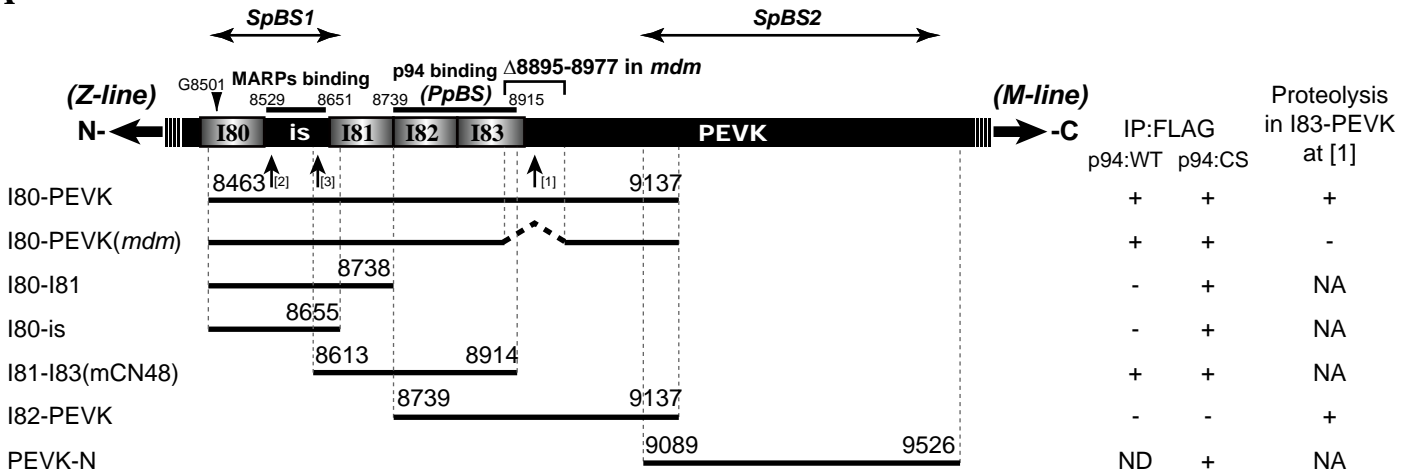
<sup>a</sup> Mice homozygous for wild type allele of *Tm*, *Tm*<sup>+/+</sup>. <sup>b</sup> Mice homozygous for *mdm* allele of *Tm*, *Tm*<sup>*mdm/mdm*</sup>. <sup>c</sup> Result of western blot analysis in Fig. 3D was summarized quantitatively.

**Table III. Expression of MARPs and MHCs**

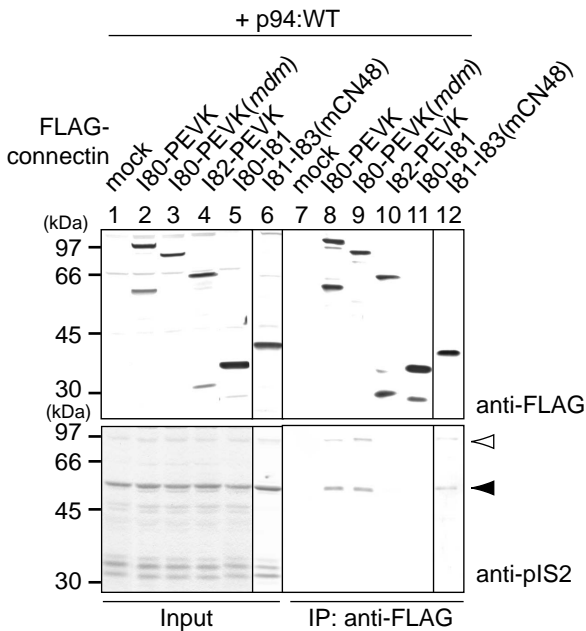
	Overall expression in cross-sectional area <sup>c</sup>		Combinations of expression at a muscle fiber level <sup>d</sup>				
	WT <sup>a</sup>	<i>mdm</i> <sup>b</sup>	<i>mdm</i>				
<b>MARP1</b>	-	+		+			+
<b>MARP2</b>	+	+++	+	+	+	+	+
<b>slow MHC</b>	+	++				+	+
<b>developmental MHC</b>	-	+	+	+			

<sup>a</sup> Mice homozygous for wild type allele of *Ttn*, *Ttn*<sup>+/+</sup>. <sup>b</sup> Mice homozygous for *mdm* allele of *Ttn*, *Ttn*<sup>*mdm/mdm*</sup>. <sup>c</sup> Expression of each protein examined by immunofluorescent study on cross sections of posterior segment of hind limbs was categorized based on the positive rate. +++ = >50%; ++ = 10-50%; + = 1-10%; - ≈ 0%. <sup>d</sup> Trend in coexpression of proteins in the same muscle fiber from *Ttn*<sup>*mdm/mdm*</sup> muscle is summarized.

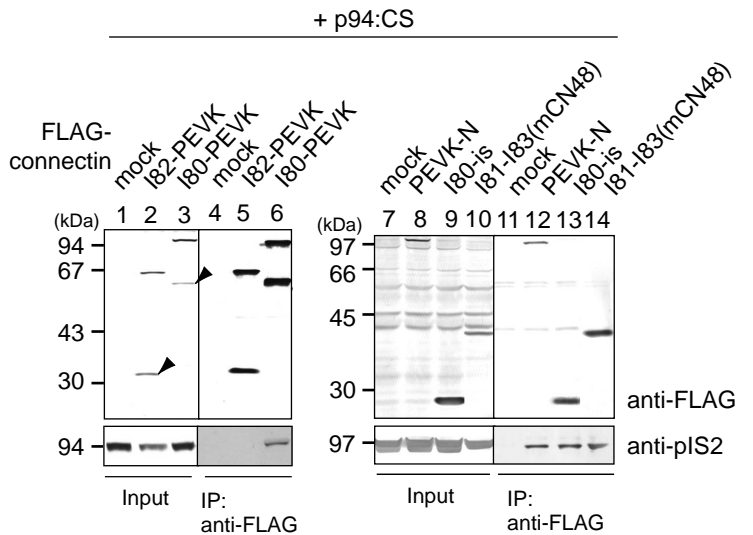
A



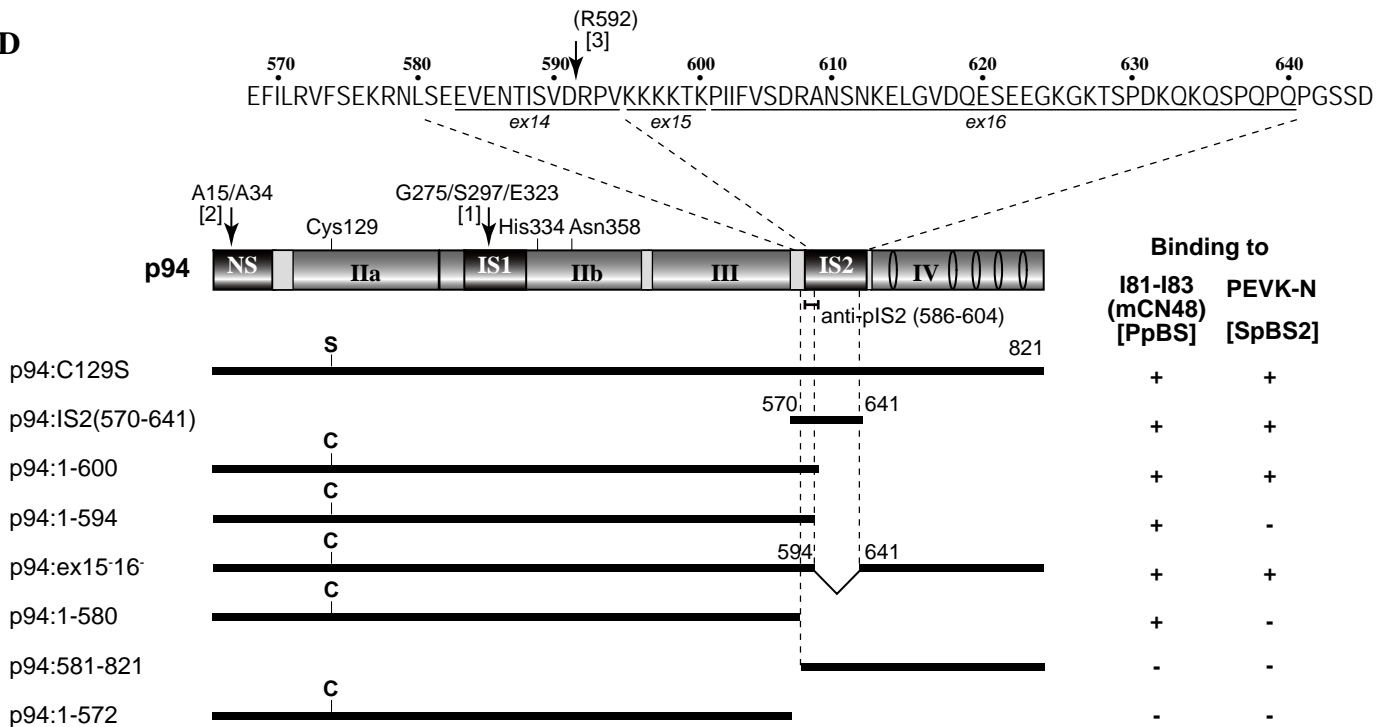
B



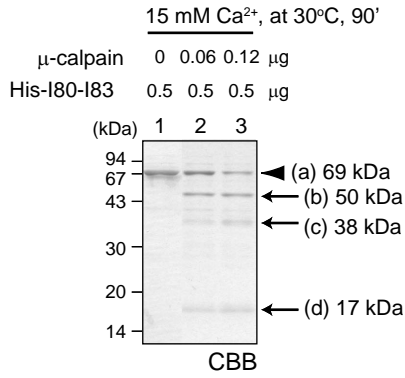
C



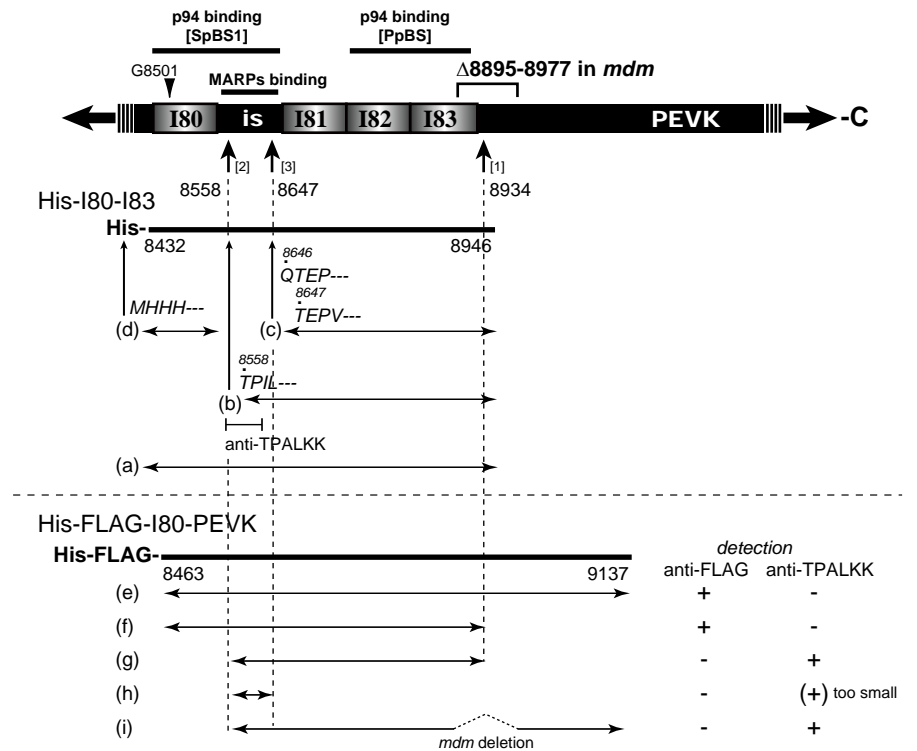
D



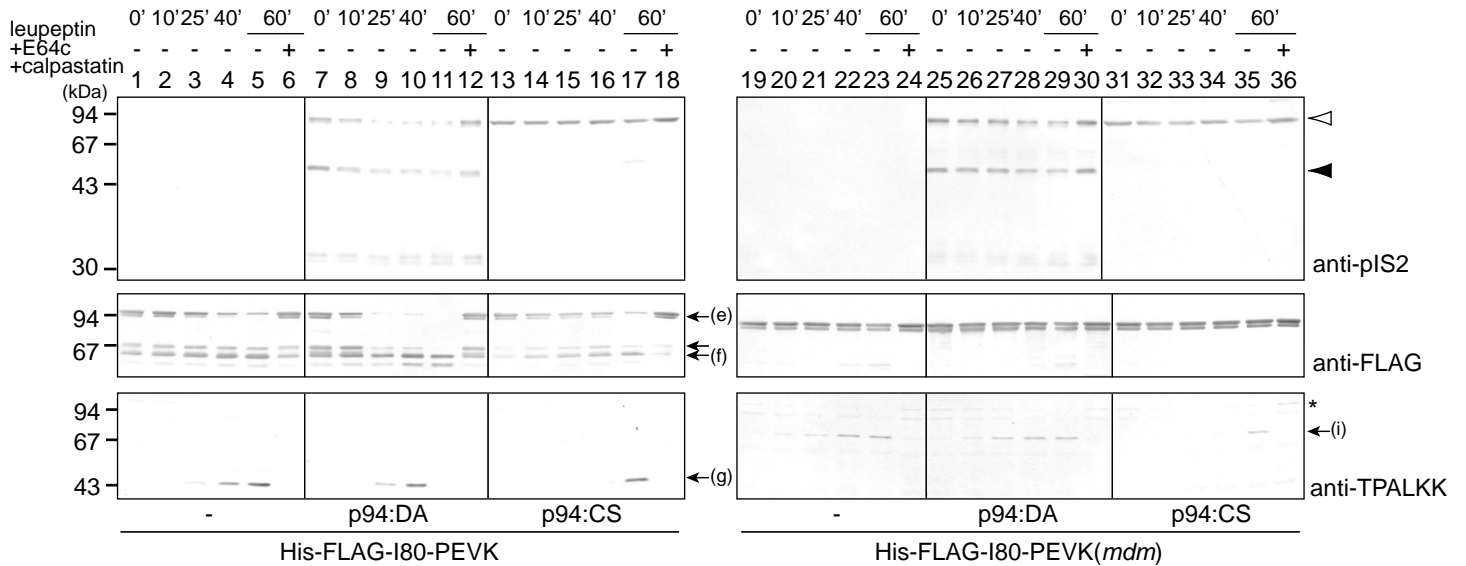
**A**



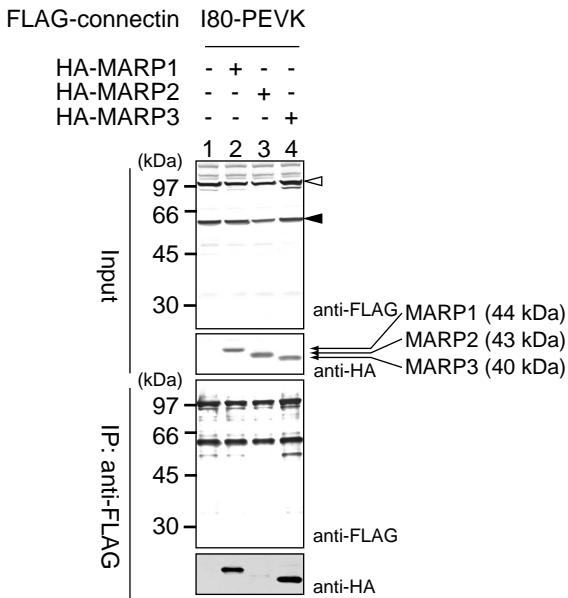
**B**



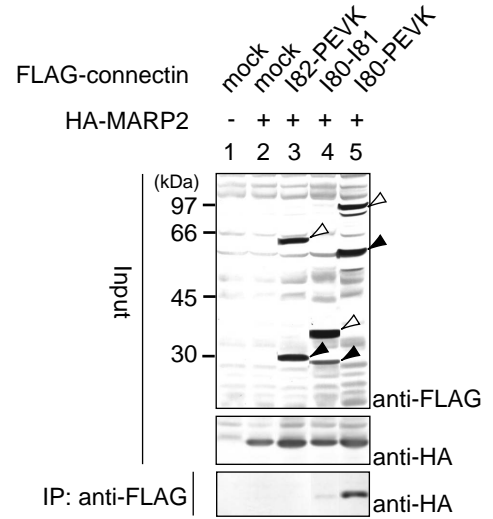
**C**



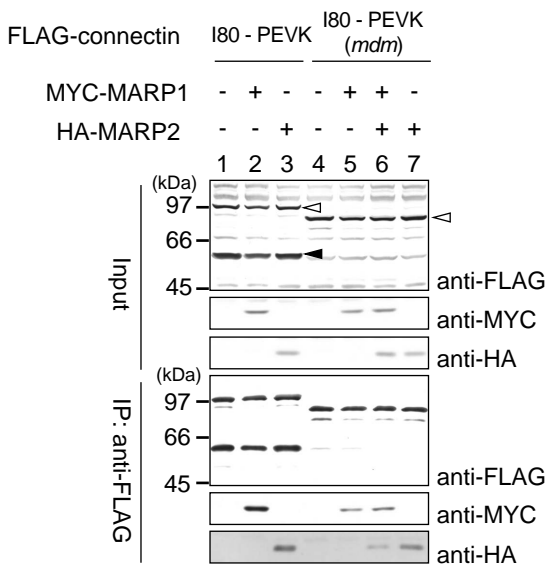
**A**



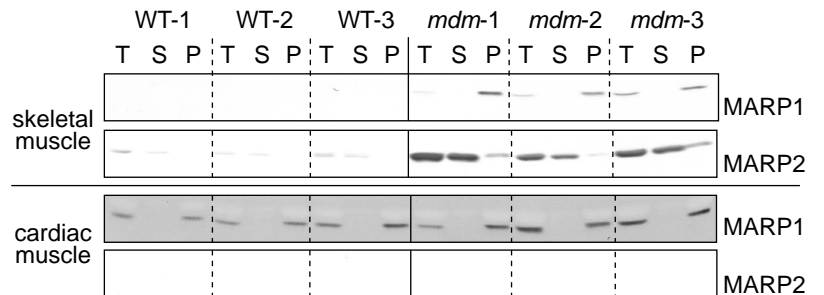
**B**

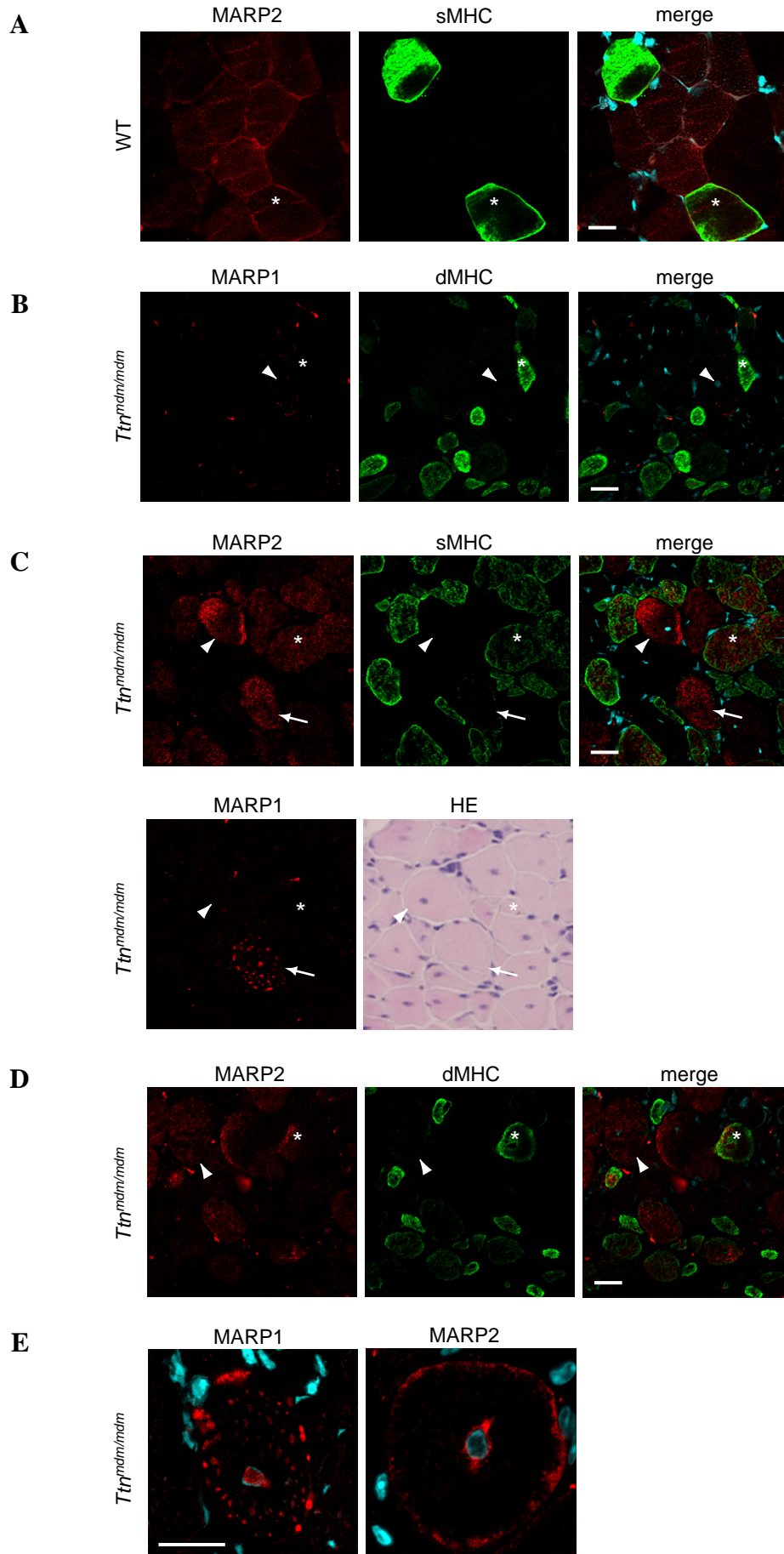


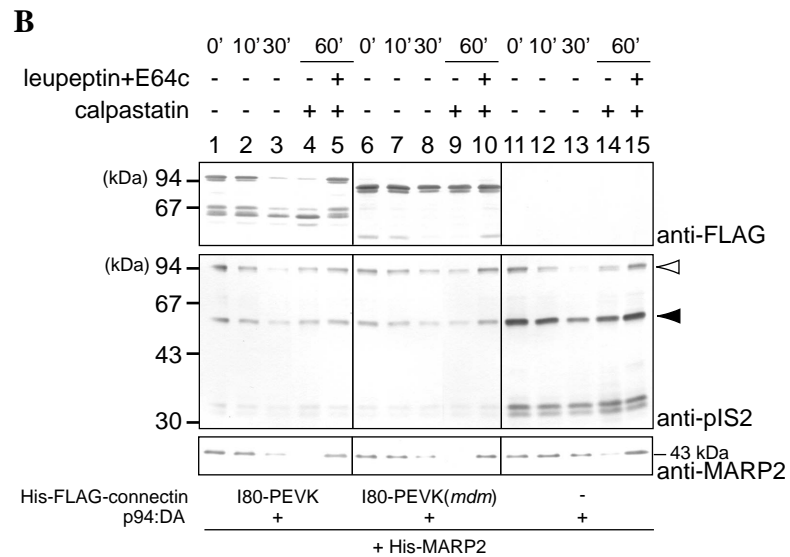
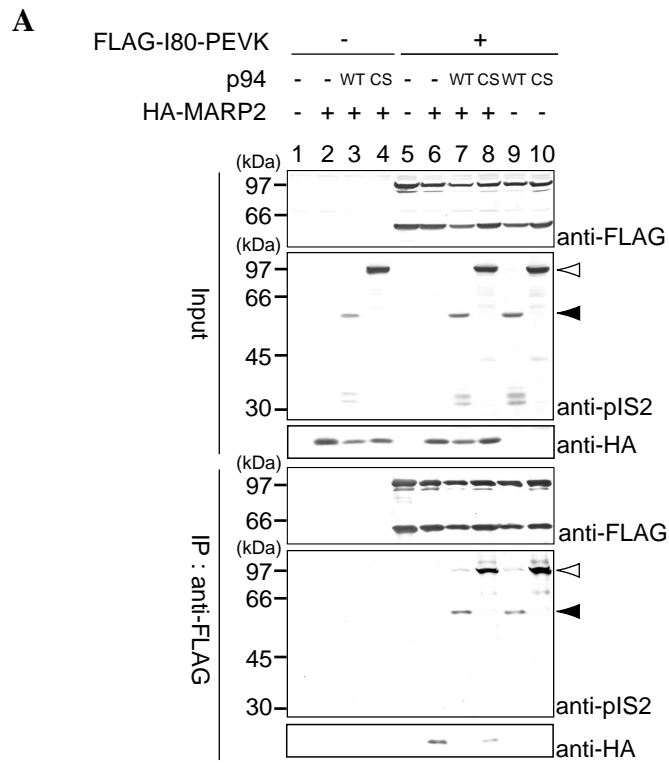
**C**



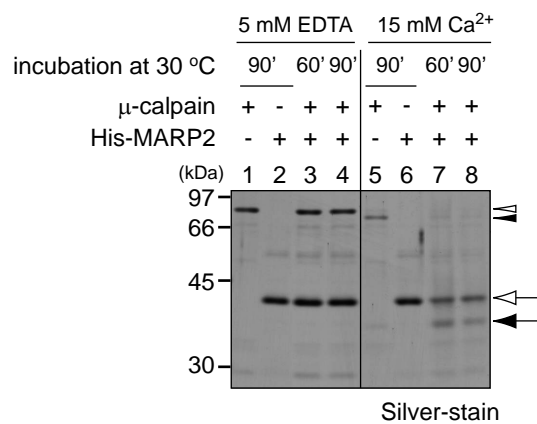
**D**



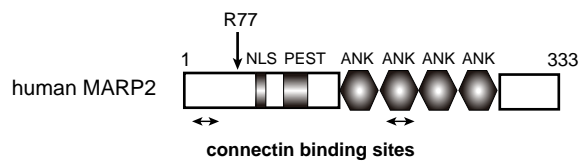




**A**



**B**



**C**

